MODELING DUST CONCENTRATION DISTRIBUTION IN A SWINE HOUSE UNDER ISOTHERMAL CONDITIONS

M. C. Puma, R. G. Maghirang, M. H. Hosni, L. J. Hagen

ABSTRACT. *A macroscopic model (Nazaroff and Cass, 1989) was used to predict dust concentration distribution in a mechanically ventilated swine nursery room under isothermal flow conditions. Four particle diameter size ranges, 0.5 to 0.9, 0.9 to 1.6, 1.6 to 2.8, and 2.8 to 5.0 μm, were considered. Effects of dust generation rate, source location, and presence/absence of obstructions (mock pigs) on dust concentration distribution were evaluated. Predicted results were compared with experimental data from full-scale laboratory tests. Based on the ASTM (1995) criteria, predicted values for the 0.5 to 0.9, 0.9 to 1.6, and 1.6 to 2.8 μm particle size ranges and total dust (0.5 to 5.0 μm) agreed well with measured values; however, measured values for the 2.8 to 5.0 μm size range were higher than predicted values. Source location significantly ($p < 0.05$) influenced the dust concentration distribution, whereas dust generation rate and presence/absence of the mock pigs did not significantly ($p < 0.05$) influence the dust distribution.*

Keywords. *Indoor air quality, Livestock buildings, Dust concentration distribution.*

High dust concentration, a prevalent air quality problem in livestock buildings, can present a significant burden to the respiratory tract of humans and animals. Dust particles also can carry microorganisms, gases, and toxins. Improved understanding of the distribution of dust particles in livestock buildings will help develop effective dust control strategies.

A recent trend in the analysis of airflow and dust transport is toward numerical modeling. Numerical modeling of dust concentration in rooms employs either macroscopic or microscopic models. Microscopic models are used to examine the details of air and contaminant movement within air spaces. These models are based on partial differential equations of fluid motion and distributed parameters. Previous studies (Maghirang and Manbeck, 1993; Maghirang et al., 1994; Worley and Manbeck, 1995) have illustrated use of microscopic models to predict air and dust concentration distribution in poultry houses.

Macroscopic models, on the other hand, are used to estimate the average value of particle parameter (usually the concentration) for a microenvironment. These models are based on control volume and lumped parameter formulations and involve ordinary differential equations of mass. The models are useful in determining flow of contaminant from one zone to another within a space through known, discrete flow paths. Liao and Feddes (1992) have successfully employed a lumped-parameter model for predicting airborne dust concentrations within a ventilated airspace based on dust generation and ventilation rates. These prediction models can be used to assess the hazards associated with indoor air quality in confined animal facilities and to evaluate proposed control measures to mitigate those hazards.

More research needs to be done on dust concentration distribution in livestock buildings. Effects of various factors such as obstruction, ventilation rate, source location, should be established. This research modeled dust concentration distribution in a mechanically ventilated, swine nursery room. Specific objectives were to:

1. Model and predict changes in concentration and fates of airborne dust, under isothermal flow conditions, in a swine nursery room.
2. Investigate the effects of dust generation rate, presence/absence of obstructions, and source location on the spatial distribution of dust concentration.
3. Validate predicted results using experimental data from full-scale laboratory tests.

MATERIALS AND METHODS

PROTOTYPE SWINE ROOM

A room air distribution chamber (7.1 m × 3.5 m × 2.4 m) (fig. 1) was designed and constructed to represent a section of a typical, mechanically ventilated, swine nursery room. The room had a cross-flow jet ventilation system with air entering through a rectangular inlet (54.6 × 24.1 cm) on one sidewall and being exhausted by a 40.6 cm diameter variable speed fan on the opposite sidewall. An expanded fiber media furnace air filter (American AirFilter International, Louisville, Ky.) was installed at the inlet to remove large particles from the incoming air.

Article was submitted for publication in November 1998; reviewed and approved for publication by the Structures & Environment Division of ASAE in August 1999.

The authors are **Manuel C. Puma**, ***ASAE Member Engineer***, Postdoctoral Research Associate, Iowa State University (formerly Graduate Research Assistant, Kansas State University); **Ronaldo G. Maghirang**, ***Member Engineer***, Associate Professor, Biological and Agricultural Engineering Department, Kansas State University, Manhattan, Kansas; **Mohammad H. Hosni**, Professor and Director, Institute for Environmental Research, Kansas State University, Manhattan, Kansas; and **Lawrence Hagen**, ***Member Engineer***, Agricultural Engineer, USDA Wind Erosion Research Unit, Manhattan, Kansas. **Corresponding author:** Dr. Ronaldo G. Maghirang, Kansas State University, 147 Seaton Hall, Manhattan, KS 66506; voice: (785) 532-2908, fax: (785) 532-5825, e-mail: rmaghir@bae.ksu.edu.

  0001-2351 / 99 / 4206-1811

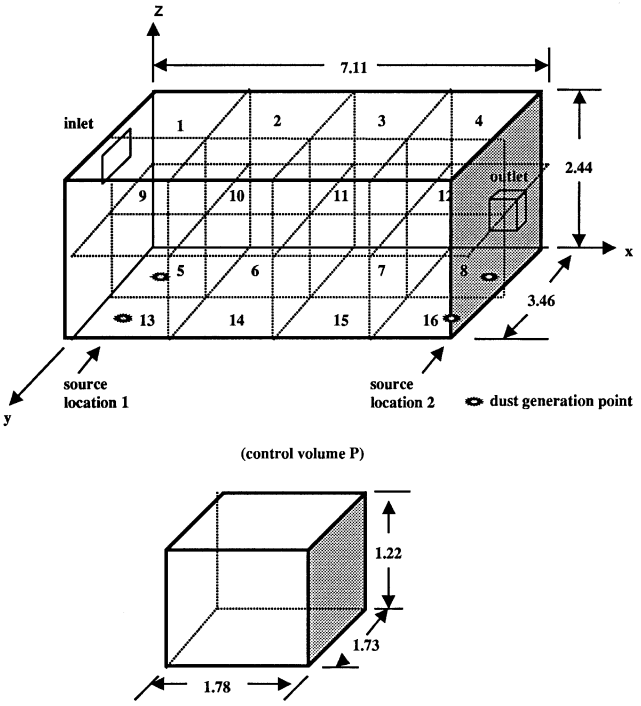

Figure 1–Schematic diagram of the prototype swine room used in the numerical and physical modeling (all units in m, not drawn to scale).

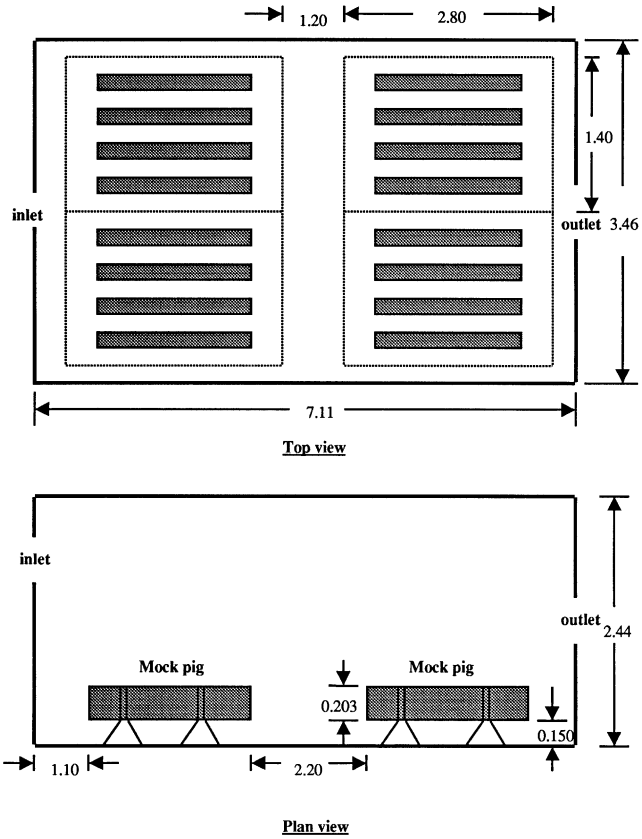

Figure 2–Layout of mock pigs in the chamber (all units in m, not drawn to scale).

The room was divided into four pens. Each pen measured 1.4 m × 2.8 m, with two pens separated from the other two by a 1.2 m alley (fig. 2). Each pen represented a space for 12 nursery pigs resulting in a stocking density of 0.33 m^2/head, which was consistent with the current floor space recommendations (0.28 to 0.37 m^2/head for nursery pigs) (MWPS, 1990). The pigs were represented by "mock pigs" which were made of galvanized steel tubes (2.80 m long and 20.3 cm in diameter) capped at both ends and supported by flat steel bars at a height of 15 cm above the floor (fig. 2). Sixteen tubes were used, with each tube representing three pigs. The mock pigs were used for test cases with obstructions and removed for test cases without obstructions.

Numerical Modeling

A macroscopic model, which was initially formulated by Nazaroff and Cass (1989) was used. The model accounted for the effects of ventilation, deposition onto surfaces, and direct emission of particles. Development and implementation of the model were presented by Puma (1998). Four particle diameter size ranges, 0.5 to 0.9, 0.9 to 1.6, 1.6 to 2.8, and 2.8 to 5.0 μm, were considered. To determine dust distribution, the room was divided into 16 control volumes; each control volume measured 1.78 m × 1.73 m × 1.22 m.

For each control volume p, the rate of change of dust mass concentration according to particle size range q was modeled using a modified version of the Nazaroff and Cass model, that is:

$$\frac{dC_{pq}}{dt} = S_{pq} - (LC)_{pq} \qquad (1)$$

where

C_{pq} = mass concentration of dust particles within size range q in control volume p (μg/m^3)
S_{pq} = rate of production of dust particles within size range q in control volume p (μg/m^3-s)
L_{pq} = rate of loss of dust particles within size range q in control volume p (s^{-1})
q = 1, 2, …, 4
p = 1, 2, …, 16

S_{pq} included direct emission inside the swine room, advective transport from the ventilation system, and coagulation of particles. Because the room was windowless and airtight, advection from outside air was neglected.

L_{pq} included particle losses to surfaces (i.e., deposition), removal by ventilation, and loss to a larger size by coagulation.

Effects of dust generation rate (high vs low), source location (near inlet vs near exhaust), and presence/absence of "mock pigs" on dust concentration distribution were evaluated (table 1). All six test cases had a ventilation rate of 0.007 m^3/s-head (18.5 air changes/h). Additionally, temperatures of inlet and inside air ranged from 24 to 27°C. Total dust generation rates were 218 to 233 μg/min in the low range and 307 to 335 μg/min in the high range (table 2). These values were determined from preliminary tests involving a dust generator, which is described below (Puma, 1998). Source location 1 was near the inlet while location 2 was near the exhaust (fig. 1). Each of the two locations had two dust generation points, one on each half

Table 1. Descriptions of test cases for the numerical and physical modeling

Test Case No.	Ventilation Rate (m^3/s-head)	Particle Generation Rate	Obstruction	Source Location*
1	0.007	Low	Without	1
2	0.007	Low	With	1
3	0.007	High	Without	1
4	0.007	High	With	1
5	0.007	High	Without	2
6	0.007	High	With	2

* 1 = source location near the inlet; 2 = source location near the exhaust.

Table 2. Dust generation rates (μg/min), based on particle size range, used for each test case

Test Case	Particle Size Range (μm)					
	(0.5-0.9)	(0.9-1.6)	(1.6-2.8)	(2.8-5.0)	Total	Low/High*
1	22.9	19.4	94.8	96.3	233.2	Low
2	16.1	15.9	88.2	97.4	217.5	Low
3	25.2	26.1	138.2	117.8	307.3	High
4	33.8	32.3	157.4	111.0	334.6	High
5	28.2	30.7	137.6	125.8	332.3	High
6	26.0	32.0	149.7	120.6	328.4	High

* Low total dust generation rate = 217.5-233.2 μg/min; high total dust generation rate range = 307.3-334.6 μg/min.

of the chamber, located at 20 cm above the floor and 50 cm from the wall.

Experimental Validation

A room air distribution chamber was used to verify predicted results. Airflow patterns were visualized using tracer smoke. A smoke gun using titanium tetrachloride (Model 15-092T-T, E. Vernon Hill, Inc., Benecia, Calif.) was used. Coplanar boundaries of the control volumes were divided into 16 grids, and flow directions were determined in each of those grids (30.5 × 43.0 cm) using a smoke gun. Velocity readings were also taken at each grid center. From the flow directions taken from each grid, the general airflow pattern in the chamber was determined (fig. 3). The airflow patterns were similar for test cases having source location 1 and 2. For test cases that had mock pigs, part of the flow near the "animal zone" was deflected by the mock pigs. However, this did not have much effect on the cross-flow ventilation rates between the lower control volumes.

A temperature-compensated, omnidirectional air velocity sensor (Model 8475, TSI, Inc., St. Paul, Minn.) was used to measure low air velocities (< 2.5 m/s) in the chamber. The sensor was placed successively at the center of each grid for 3 min. Voltage measurements were stored and converted to velocity values using a data logger (Model 21X, Campbell Scientific, Inc., Logan, Utah). From the measured air velocities and cross-sectional areas of the grids, cross-flow ventilation rates between the control volumes were established.

A dust generator (Model NBS, F. E. Wiedeman & Sons, Ossipee, N.H.) was used to generate a known mass of dust into the chamber. The equipment was developed at the former National Bureau of Standards, and was originally used for generating soil particles for wind erosion research. Dust is placed in a hopper where it flows down due to gravity. It is then caught between the teeth of a vertically

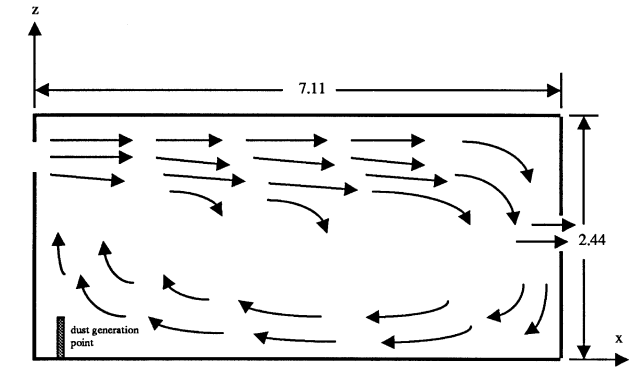

(a) Without obstruction

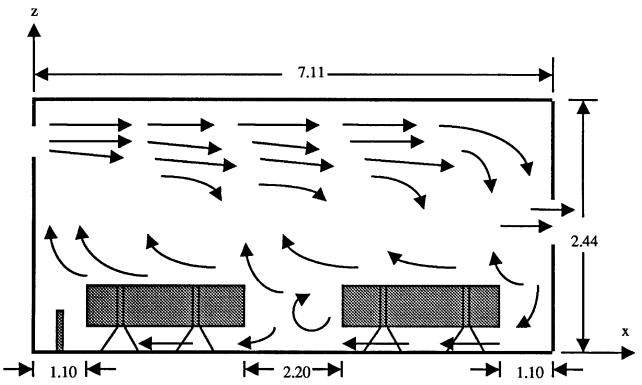

(b) With obstruction

Figure 3–General airflow pattern for the isothermal test cases (Q = 0.331 m^3/s); (a) without obstruction, (b) with obstruction (all units in m).

rotating gear and drawn up a feed tube by suction. Dust particles were emitted into the air stream through two plastic tubes, one on each side of the chamber, with the end of each tube set at 20 cm above the floor. Cornstarch powder was chosen as the test dust material. A pycnometer, a standard equipment for measuring densities of powder, showed that the mean particle density was 1.6 g/cm^3.

A microprocessor-controlled optical particle counter (OPC) (Model 200, MET ONE, Inc., Grants Pass, Oreg.), which measured number of particles in the size ranges 0.5 to 0.9, 0.9 to 1.6, 1.6 to 2.8, 2.8 to 5.0, 5.0 to 10.0, and >10.0 μm, was used. Because the study involved respirable dust particles, only the first four particle size ranges were considered in subsequent data analyses. The OPC was connected to a multiple sampling port/manifold system (Model 231, MET ONE, Inc., Grants Pass, Oreg.) to enable automatic measurements from 16 locations. Preliminary measurements indicated that airflow patterns and dust concentration distribution in the room were symmetrical about the longitudinal dimension (along the inlet air direction). Hence, measured values from eight control volumes, or in only half of the chamber, were considered. Sampling was done at the center of each control volume using plastic tubing of 9.5 mm internal diameter connected to the multiple sampling port. The sampling tubes were held at the center of the control volumes by thin, stiff G. I. wires attached to the floor and ceiling on each end. From the multiple sampling port, air was drawn through a 2.0 m

length of plastic tubing, which brought the air sample to the OPC. Sampling time was 15 s for each control volume, and sampling interval between any two control volumes was 15 s. Preliminary tests indicated that 15 s was the shortest time possible to accurately measure dust concentration from a control volume, considering the average length of the sampling tubes used. The shortest sampling time for each control volume and between each control volume were considered to complete the measurement of dust concentration from the 16 control volumes within the shortest time period. It took 8 min to get the concentration measurements from all of the 16 control volumes during each reading. Particle concentrations were measured at 15-min intervals starting with the beginning of dust generation until attainment of steady-state concentration, which usually took 1.5 h.

Thermocouples (Type T, Omega Engineering, Inc., Stamford, Conn.) were used to monitor air temperatures at the center of each control volume, at the inlet, the exhaust, and outside the chamber. Thermocouples were also embedded about 1 mm deep and at the center of each wall and ceiling or floor area bounding each control volume to measure the surface temperatures. Temperatures were measured every 5 min, and averages of 30-min periods were recorded using a data logger (Model 21X, Campbell Scientific Inc., Logan, Utah).

The inside surfaces of the chamber were cleaned thoroughly before each test. A test was started only when the dust concentrations in the control volumes were at levels that are within 5% of the outdoor concentrations. Outdoor and exhaust dust concentrations were monitored throughout the tests.

Dust generation rates (table 2) were determined from preliminary tests. A steady-state mass balance of the whole chamber was done using:

$$C_i \times Q + G = C \times Q + R \quad (2)$$

where

C_i = dust mass concentration at the inlet ($\mu g/m^3$)
C = steady-state dust mass concentration in the chamber ($\mu g/m^3$)
Q = ventilation rate (m^3/s)
G = dust particle generation rate ($\mu g/s$)
R = dust removal rate (mainly by deposition to surfaces) ($\mu g/s$)

C_I and Q were measured. Dust removal rate, R, was estimated. Only the deposition on the floor was considered for the dust removal rate because deposition on the walls and ceilings were much smaller than deposition on the floor. The average of the dust mass concentrations measured from the control volumes was used as the steady-state dust mass concentration value, C. Dust generation rate, G, was then calculated using equation 2.

Data Analyses

Measured particle counts were first converted to number concentrations (particles/cm^3) by dividing particle counts with the product of the airflow rate of the OPC (4×10^{-4} m^3/s) and the sampling time of 15 s. Then, the number concentrations were converted to mass concentrations ($\mu g/m^3$) by multiplying the number concentrations with the mass of the particle. Mass of the particle was determined using the average diameter for each particle size range to compute the volume and then multiplying the volume with the measured particle density. Uniform particle density distribution was assumed. Predicted and measured dust mass concentrations were normalized using the procedure suggested by Kato and Murakami (1995):

$$C_{pq}^*(t) = \frac{[C_{pq}(t) - C_{iq}(t)]\,Q}{G_q(t) - C_{oq}(t)\,Q} \quad (3)$$

where

$C_{pq}^*(t)$ = normalized mass concentration of particles within size range q in control volume p at time t (dimensionless)
$C_{pq}(t)$ = mass concentration of particles within size range q in control volume p at time t ($\mu mg/m^3$)
$C_{iq}(t)$ = measured concentration of particles within size range q at the inlet at time t ($\mu g/m^3$)
$G_q(t)$ = dust generation rate within size range q in control volume p at time t ($\mu g/s$)
$C_{oq}(t)$ = mass concentration of particles within size range q at the exhaust at time t ($\mu g/m^3$)
Q = ventilation rate (m^3/s)

Measured and predicted values for the different test cases were compared. Agreement between measured and predicted values provided an indication of the model's ability in predicting airborne dust concentrations. Quantitative indicators of the general agreement between the predicted (C_p) and measured/observed (C_o) values were used to assess model performance. The following statistical indices were used (ASTM, 1995): correlation coefficient (r), slope (b) and intercept (a) of the best-fit line of regression between C_p and C_o, normalized mean square error (NMSE), fractional bias (FB) of the mean concentrations, and a similar index of bias (FS) based on the variance (σ^2) of the concentration.

NMSE, a measure of the magnitude of prediction error relative to C_p and C_o, was calculated using:

$$NMSE = \frac{\overline{(C_p - C_o)^2}}{[(C_{om})(C_{pm})]} = \frac{\Sigma \frac{(C_{pi} - C_{oi})^2}{n}}{[(C_{om})(C_{pm})]} \quad (4)$$

where

C_{pm} = mean of normalized predicted values (dimensionless)
C_{om} = mean of normalized observed values (dimensionless)
n = number of predicted or observed values

The normalized or fractional bias (FB) was calculated using:

$$FB = \frac{2 \times (C_{pm}) - (C_{om})}{(C_{pm}) + (C_{om})} \quad (5)$$

The bias based on the variance, FS, was calculated as:

$$FS = \frac{2 \times \left(\delta_p^2 \times C_{pm} - \delta_o^2 \times C_{om}\right)}{\left(\delta_p^2 \times C_{pm} + \delta_o^2 \times C_{om}\right)} \quad (6)$$

where

δ_p^2 = variance of the predicted values

δ_o^2 = variance of the observed values

ASTM (1995) suggested the following values as indications of adequate model performance: $r \geq 0.90$, $0.75 \leq b \leq 1.25$, $a \leq 0.25C_{om}$, NMSE ≤ 0.25, FB ≤ 0.25, and FS ≤ 0.50. C_{om} was the mean measured mass concentration for each test case. The last six paired set of the normalized predicted and measured dust mass concentration values (from the first 15 min of the simulation or measurement until the steady-state levels were reached in one and a half hours) were used in linear regression and correlation analysis to determine r, b, a, and to compute for NMSE, FB, and FS.

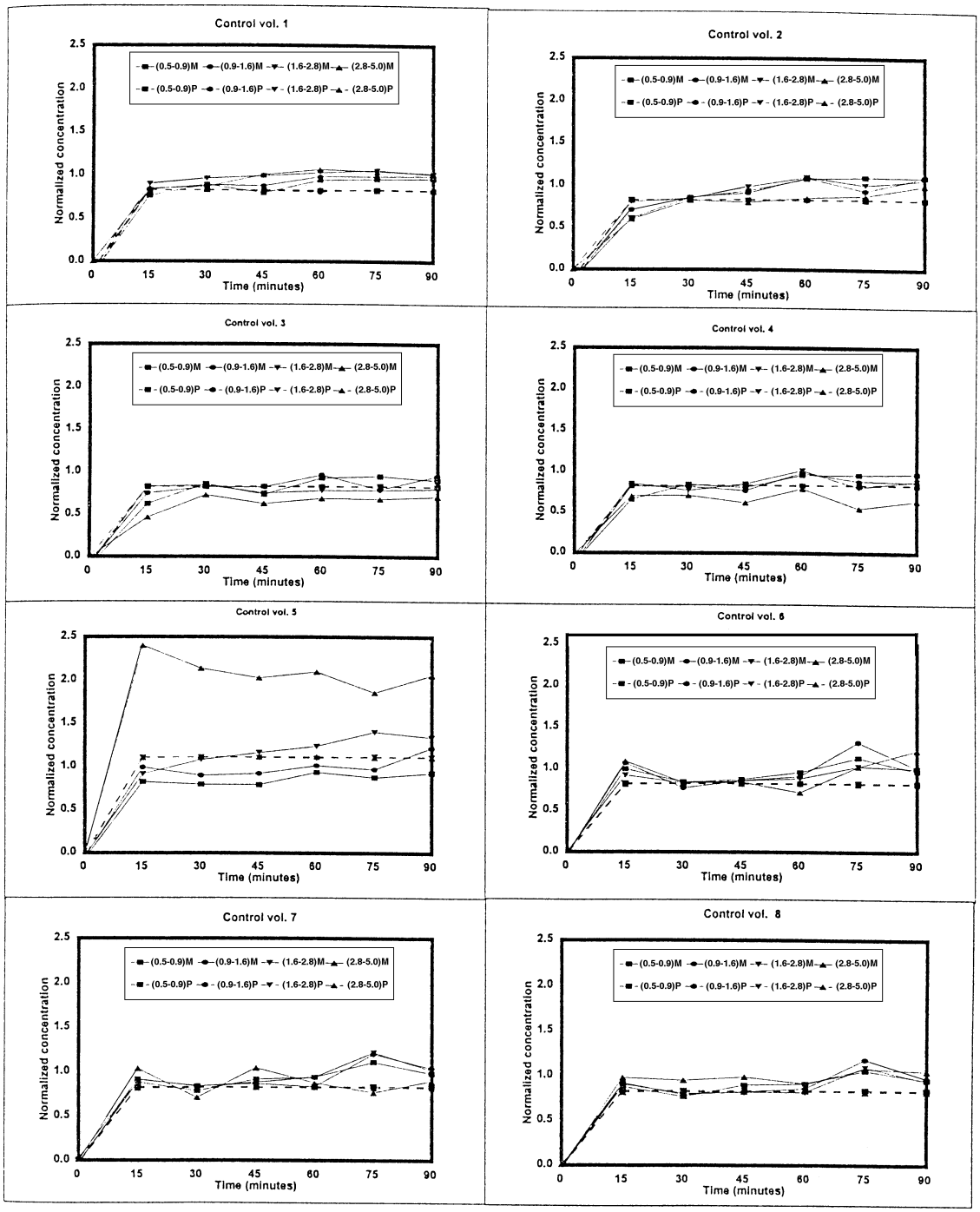

Figure 4–Comparison of predicted and measured dust mass concentrations (by particle size range) for each control volume (test case 1). Broken lines represent predicted values, solid lines represent measured values.

Comparison of results between test cases 1 and 2, 3 and 4, and 5 and 6 indicated the effects of the presence of mock pigs. Comparisons between test cases 1 and 3 and between 2 and 4 showed the effects of dust generation rate. Comparisons between test cases 3 and 5 and 4 and 6 indicated the influence of dust source location.

Analysis of Experimental Uncertainties

Uncertainties in measurements of dust concentration, flow rate, air speed, and temperature were estimated using the analytical solution-approximation method (Puma, 1998). Uncertainties in the measurements of dust mass concentrations were 6.5% of the actual measured values for both the 0.5 to 0.9 and the 0.9 to 1.6 μm particle size ranges, 15.6% for 1.6 to 2.8 μm, and 25.3% for the 2.8 to 5.0 μm. Uncertainty in airflow measurement was ± 2.0%. Uncertainties in airspeed measurements were +12%/–23% (+0.05/–0.07 m/s). Uncertainties in temperature measurements were ± 1.0°C.

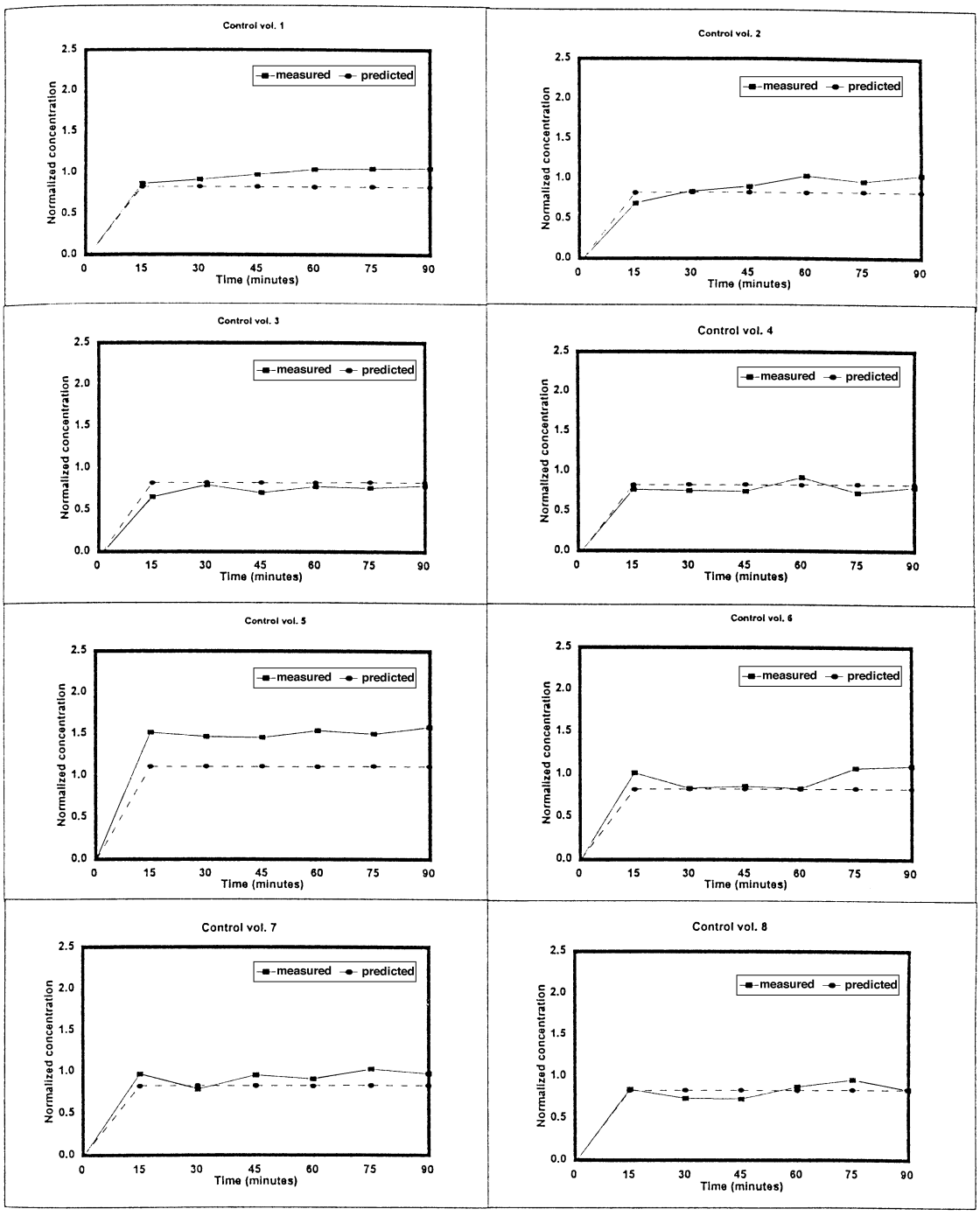

Figure 5–Comparison of predicted and measured dust mass concentrations (total dust) for each control volume (test case 1). Broken lines represent predicted values, solid lines represent measured values.

RESULTS AND DISCUSSION

PREDICTED VERSUS MEASURED DUST CONCENTRATIONS

The normalized predicted and measured concentrations, by particle size range, for test case 1 (dust source location 1, no mock pigs) are shown in figure 4. Predicted concentrations immediately increased from the initial values to levels approximating the steady-state values after the first 15 min of the simulation. Values then increased until the steady-state levels were reached in one and a half hours. Measured dust concentrations followed the same trends as the predicted values. Predicted and measured values agreed reasonably well, especially for the three smaller particle sizes (0.5 to 0.9, 0.9 to 1.6, 1.6 to 2.8 μm). However, measured concentrations of the 2.8 to 5.0 μm were much higher than predicted values at control volume 5. This discrepancy between the predicted and measured values

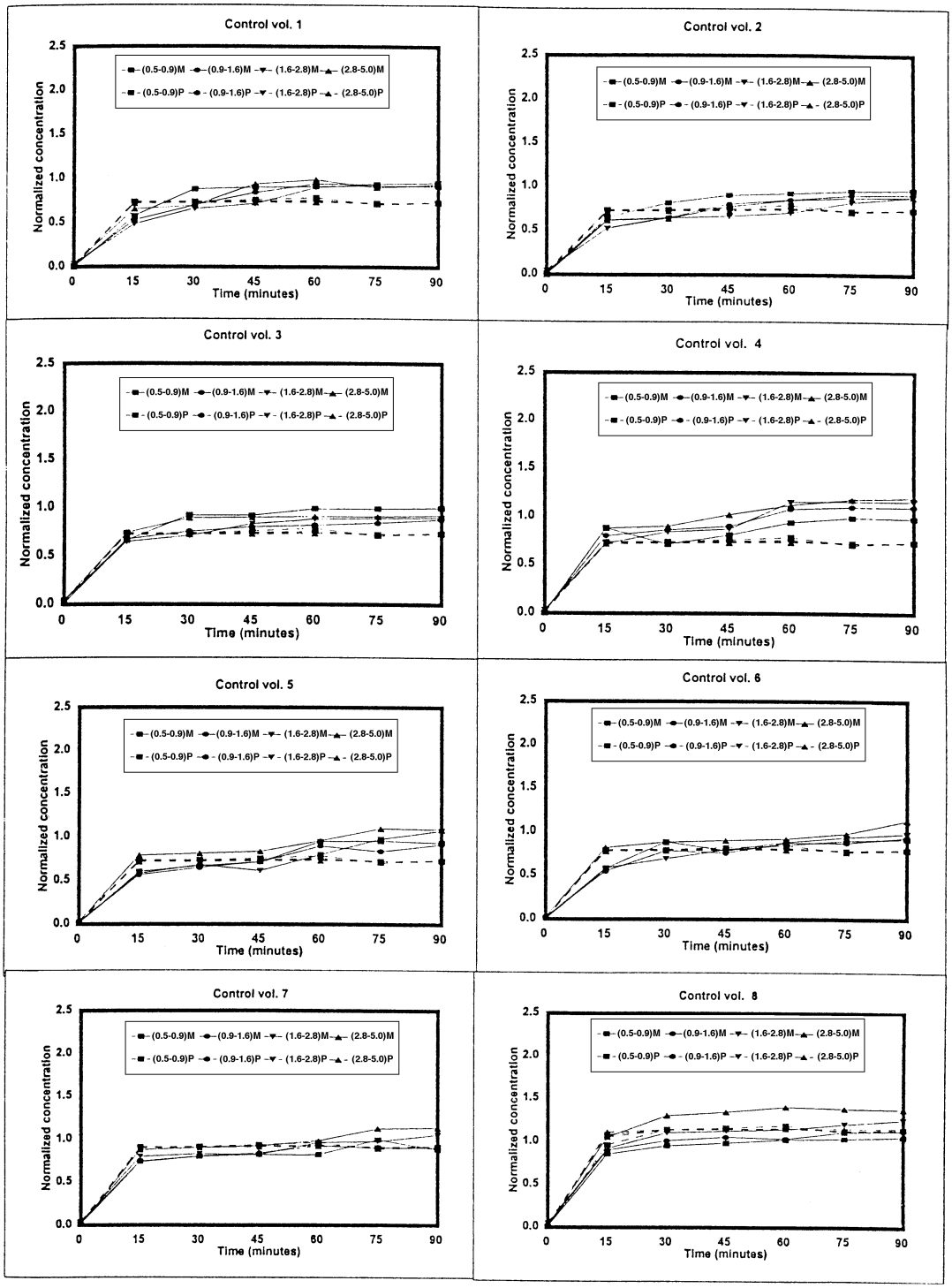

Figure 6–Comparison of predicted and measured dust mass concentrations (by particle size range) for each control volume (test case 5). Broken lines represent predicted values, solid lines represent measured values.

Table 3. Model performance statistics for test case 1

Control Volume Number	Particle Size Range (μm)	Statistics: Correlation Coefficient r	Regression Slope b	Regression Intercept a	25% of Mean C_o*	NMSE†	FB‡	FS§
1	(0.5-0.9)	0.94	0.78	0.07	0.2	0.06	−0.14	0.13
	(0.9-1.6)	0.95	0.78	0.05	0.2	0.06	−0.17	0.09
	(1.6-2.8)	0.94	0.7	0.06	0.22	0.11	−0.26	−0.1
	(2.8-5.0)	0.94	0.76	0.09	0.22	0.08	−0.22	−0.06
	Total	0.94	0.72	0.07	0.22	0.09	−0.22	−0.05
2	(0.5-0.9)	0.91	0.73	0.11	0.2	0.08	−0.15	0.07
	(0.9-1.6)	0.92	0.75	0.09	0.2	0.07	−0.15	0.08
	(1.6-2.8)	0.96	0.79	0.04	0.21	0.06	−0.17	0.1
	(2.8-5.0)	0.89	0.76	0.15	0.18	0.05	−0.03	0.26
	Total	0.94	0.79	0.08	0.2	0.04	−0.11	0.17
3	(0.5-0.9)	0.95	0.9	0.06	0.17	0.02	−0.01	0.41
	(0.9-1.6)	0.97	0.92	0.03	0.18	0.01	−0.03	0.4
	(1.6-2.8)	1	1.02	0.01	0.17	0	0.04	0.57
	(2.8-5.0)	0.95	1.13	0.08	0.14	0.08	0.24	0.49
	Total	0.99	1.07	0.02	0.16	0.02	0.1	0.69
4	(0.5-0.9)	0.96	0.89	0.06	0.18	0.02	−0.04	0.35
	(0.9-1.6)	0.98	0.94	0.02	0.18	0.01	−0.03	0.41
	(1.6-2.8)	0.97	0.92	0.03	0.18	0.01	−0.04	0.38
	(2.8-5.0)	0.96	1.14	0.06	0.14	0.07	0.22	0.91
	Total	0.98	1.01	0.03	0.17	0.01	0.06	0.59
5	(0.5-0.9)	0.99	1.24	0.04	0.18	0.08	0.26	1.01
	(0.9-1.6)	0.97	1.03	0.06	0.21	0.02	0.1	0.67
	(1.6-2.8)	0.95	0.84	0.1	0.25	0.03	−0.07	0.26
	(2.8-5.0)	0.98	0.51	0.03	0.45	0.5	−0.62	−0.62
	Total	1	0.9	0	0.32	0.11	−0.31	−0.14
6	(0.5-0.9)	0.97	0.82	0.04	0.21	0.04	−0.15	0.14
	(0.9-1.6)	0.92	0.7	0.11	0.21	0.08	−0.18	−0.01
	(1.6-2.8)	0.98	0.86	0.03	0.2	0.02	−0.11	0.22
	(2.8-5.0)	0.9	0.71	0.12	0.2	0.07	−0.16	0.03
	Total	0.96	0.8	0.06	0.2	0.04	−0.14	0.13
7	(0.5-0.9)	0.97	0.83	0.04	0.2	0.03	−0.12	0.2
	(0.9-1.6)	0.94	0.77	0.09	0.2	0.04	−0.13	0.1
	(1.6-2.8)	0.95	0.78	0.06	0.21	0.05	−0.16	0.09
	(2.8-5.0)	0.94	0.8	0.1	0.19	0.03	−0.08	0.2
	Total	0.98	0.79	0.03	0.2	0.02	−0.12	0.19
8	(0.5-0.9)	0.97	0.87	0.04	0.19	0.02	−0.08	0.28
	(0.9-1.6)	0.95	0.8	0.08	0.2	0.03	−0.1	0.19
	(1.6-2.8)	0.96	0.86	0.05	0.19	0.02	−0.07	0.28
	(2.8-5.0)	0.99	0.8	0.03	0.21	0.04	−0.18	0.06
	Total	0.97	0.85	0.03	0.2	0.02	−0.11	0.22

* C_o = mean measured dust concentration.
† NMSE = normalized mean square error.
‡ FB = normalized or fractional bias.
§ FS = bias based on the variance.

could have been due to higher error in measurements of the concentrations of that particle size range (≈ 25.3%). Additionally, at control volume 5 (where the source was located), the concentration of the large particles may not have been uniform throughout the control volume.

Predicted and measured values of the total dust (0.5 to 5.0 μm) concentrations for test case 1 are shown in figure 5. Good agreements between the predicted and measured total dust concentrations are apparent for most control volumes, except for control volume 5, where measured values were much higher than the predicted values. This was due to the contribution of the high concentration of the 2.8 to 5.0 μm particles to the measured total dust concentration at that control volume.

The indices for evaluating the adequacy of the predictive model are listed in table 3. For test case 1, r values were all higher than 0.9. Regression intercepts, a, were all lower than 25% of the mean measured concentrations. FB values were all below 0.25, and NMSE values had only one value higher than 0.25. Several values of the regression slope, b, were below 0.75, and some FS values higher than 0.5. Overall, the criteria for the adequacy of the statistical indices were generally satisfied, indicating that predicted and measured values were in good agreement.

Comparison of predicted and measured values of total dust for test cases 2 to 4 yielded the same trends, that is, predicted values agreed well with measured values.

Predicted and measured values for test case 5 (source location 2, no mock pigs) are shown in figure 6 (four particle diameter size ranges) and figure 7 (total dust). For the upper control volumes, measured values were slightly higher than the predicted values of all four particle size ranges. For the lower control volumes, agreements between measured and predicted values were closer. Predicted and measured values of the total dust (0.5 to 5.0 μm) concentrations for test case 5 showed close agreement (fig. 7) for most control volumes, but not control volumes 4 and 8. Note that control volume 8 was the dust source location, and control volume 4 was directly above it. Statistical indices for assessing the model performance are given in table 4. Several values of the regression slope, b, especially those for the upper control volumes (1 to 4) and for control volume 5, were less than 0.75 indicating that predicted values were lower than the measured values for those control volumes. All the other indices were well within the acceptable limits. Overall, good agreements between predicted and measured values also existed for test case 5. For test case 6 (source location 2, with mock pigs), measured and predicted values also agreed reasonably well.

Effects of Mock Pigs, Dust Generation Rates, and Source Location

Comparisons of results between test cases 1 and 2, 3 and 4, and 5 and 6 revealed that the mock pigs had only slight effects on dust concentration distribution in the chamber (table 5). Note that the mock pigs occupied only a small portion (2.3%) of the control volumes, such that airflow between the control volumes were not affected much. Furthermore, the general airflow direction in the chamber was parallel with the mock pigs so that they provided minimal resistance to the air movement.

Comparisons of results between test cases 1 and 3 and 2 and 4 showed that levels of dust generation rate also had only slight effects on dust concentration distribution (table 6). Actual values of dust concentrations (in $\mu g/m^3$) were higher for test cases with higher dust generations than those with lower dust generation rates, but, normalized values were almost the same for both test cases.

Comparisons of the results between test cases 3 and 5 and those between test cases 4 and 6 indicated that source location affected the dust concentration distribution (table 7). For both source locations, predicted and measured values were higher at or near the source location (i.e., control volume 5 for source location 1 and control volume 8 for source location 2) than in the other control volumes. Test cases that had source location 1 (test cases 1 to 4) showed small differences in the concentrations of all the other control volumes, because the dominant airflow in the chamber consisting of a big, clockwise circulating eddy caused good mixing and distribution of dust particles in the chamber, except at the dust source location. This dust source location was near the inlet where the circulating airflow originated. For test cases which had source location 2 (test cases 5 and 6), decreasing airflow and increasing distance from the dust source location (control volume 8) of control volumes 7, 6 and 5 caused the pattern of decreasing dust concentrations for those control volumes.

Predicted values for all test cases indicated that ventilation was the dominant dust removal mechanism, accounting for 91 to 98% of total dust (0.5 to 5.0 μm) removed. Deposition of particles on wall, ceiling, and floor surfaces (2 to 9%) was small, and effects of coagulation (≈ 0%) were negligible. Predicted particle deposition on surfaces of the mock pigs was also small. Note that the model did not consider the characteristics of the surface in predicting the amount of particle deposition so that effects of the surface characteristics of the steel tubes were not considered.

CONCLUSIONS

The following conclusions were drawn from this research:

1. Source location significantly ($p < 0.05$) influenced the dust concentration distribution; dust

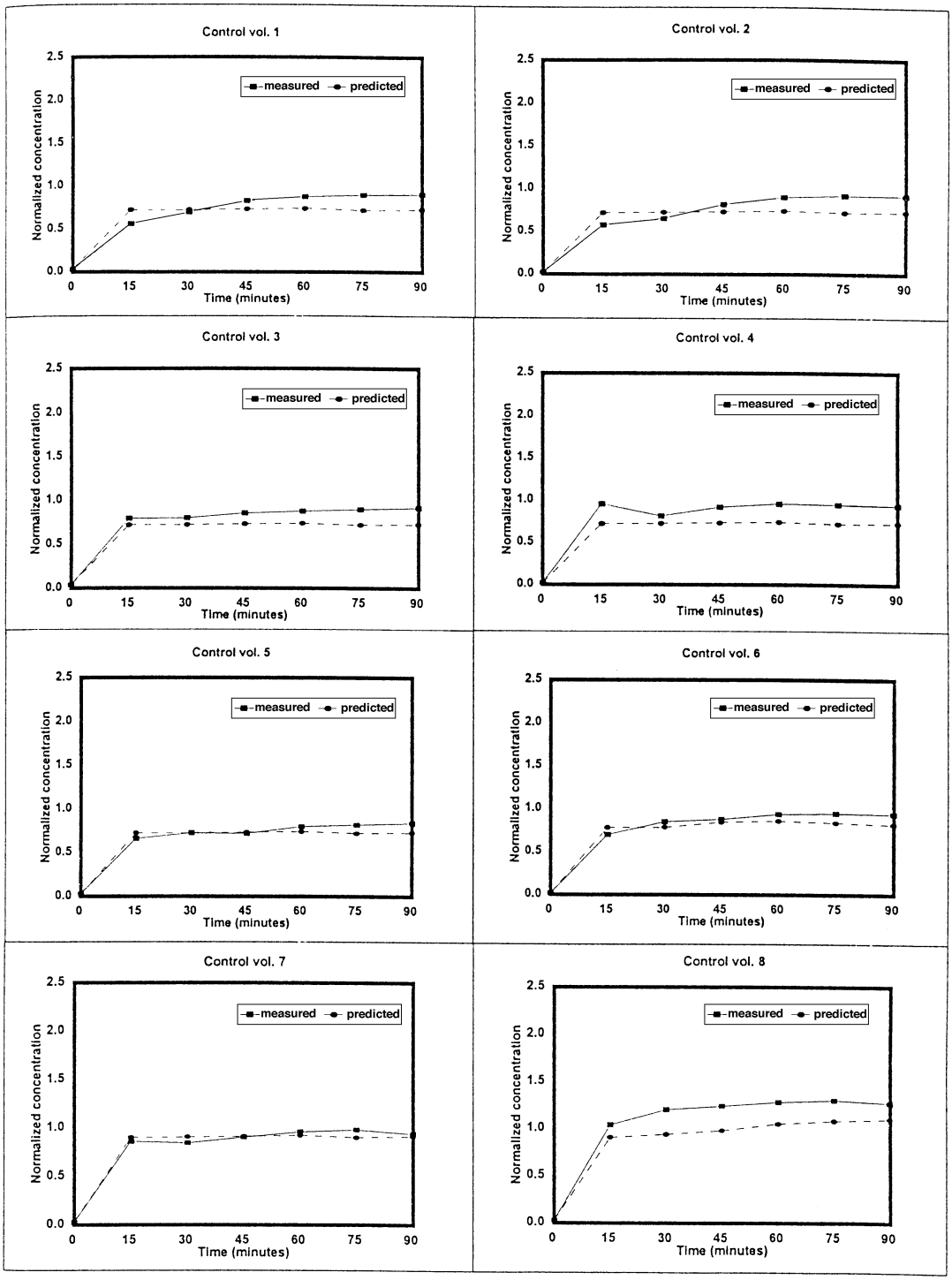

Figure 7–Comparison of predicted and measured dust mass concentrations (total dust) for each control volume (test case 5). Broken lines represent predicted values, solid lines represent measured values.

Table 4. Model performance statistics for test case 5

Control Volume Number	Particle Size Range (μm)	Statistics: Correlation Coefficient r	Regression Slope b	Regression Intercept a	25% of Mean C_o*	NMSE†	FB‡	FS§
1	(0.5-0.9)	0.93	0.76	0.08	0.18	0.05	−0.13	0.11
	(0.9-1.6)	0.9	0.71	0.14	0.18	0.06	−0.1	0.09
	(1.6-2.8)	0.85	0.68	0.18	0.17	0.06	−0.06	0.13
	(2.8-5.0)	0.93	0.76	0.09	0.18	0.06	−0.16	0.03
	Total	0.91	0.73	0.11	0.19	0.11	−0.19	−0.16
2	(0.5-0.9)	0.95	0.77	0.07	0.19	0.05	−0.15	0.09
	(0.9-1.6)	0.93	0.81	0.09	0.17	0.03	−0.07	0.24
	(1.6-2.8)	0.9	0.85	0.11	0.15	0.03	0.04	0.44
	(2.8-5.0)	0.94	0.84	0.07	0.16	0.03	−0.06	0.28
	Total	0.94	0.82	0.08	0.2	0.15	−0.22	−0.25
3	(0.5-0.9)	0.94	0.78	0.07	0.2	0.07	−0.2	−0.02
	(0.9-1.6)	0.97	0.88	0.04	0.17	0.02	−0.07	0.29
	(1.6-2.8)	0.95	0.81	0.07	0.18	0.03	−0.1	0.19
	(2.8-5.0)	0.98	0.79	0.03	0.19	0.05	−0.19	0.04
	Total	0.97	0.79	0.05	0.23	0.25	−0.38	−0.47
4	(0.5-0.9)	0.95	0.77	0.06	0.19	0.06	−0.17	0.06
	(0.9-1.6)	0.95	0.67	0.07	0.21	0.12	−0.28	−0.17
	(1.6-2.8)	0.9	0.59	0.13	0.21	0.15	−0.29	−0.27
	(2.8-5.0)	0.96	0.62	0.06	0.23	0.18	−0.36	−0.32
	Total	0.95	0.66	0.08	0.26	0.41	−0.5	−0.61
5	(0.5-0.9)	0.9	0.75	0.12	0.17	0.05	−0.08	0.17
	(0.9-1.6)	0.91	0.79	0.11	0.16	0.04	−0.04	0.27
	(1.6-2.8)	0.84	0.65	0.19	0.17	0.08	−0.08	0.08
	(2.8-5.0)	0.94	0.68	0.08	0.2	0.1	−0.25	−0.13
	Total	0.91	0.72	0.12	0.19	0.12	−0.21	−0.18
6	(0.5-0.9)	0.93	0.86	0.09	0.18	0.03	−0.02	0.36
	(0.9-1.6)	0.92	0.84	0.11	0.17	0.03	0	0.37
	(1.6-2.8)	0.91	0.81	0.12	0.17	0.03	−0.03	0.3
	(2.8-5.0)	0.97	0.78	0.05	0.2	0.05	−0.17	0.05
	Total	0.94	0.83	0.08	0.21	0.08	−0.19	−0.06
7	(0.5-0.9)	0.96	1.02	0.05	0.18	0.02	0.09	0.66
	(0.9-1.6)	0.98	1.04	0.03	0.18	0.01	0.07	0.64
	(1.6-2.8)	0.96	0.93	0.06	0.2	0.01	0	0.45
	(2.8-5.0)	0.97	0.86	0.05	0.21	0.02	−0.08	0.26
	Total	0.97	0.96	0.04	0.22	0.06	−0.13	0.07
8	(0.5-0.9)	0.99	1.13	0.01	0.21	0.02	0.13	0.78
	(0.9-1.6)	0.99	1.06	0.02	0.22	0.01	0.08	0.66
	(1.6-2.8)	0.98	0.95	0.05	0.24	0.01	0	0.47
	(2.8-5.0)	0.98	0.83	0.05	0.28	0.03	−0.14	0.15
	Total	0.98	0.98	0.05	0.24	0.03	0.03	0.45

* C_o = mean measured dust concentration.
‡ FB = normalized or fractional bias.
† NMSE = normalized mean square error.
§ FS = bias based on the variance.

Table 5. Comparison of the means of normalized total dust concentrations between test cases 1 and 2, 3 and 4, and 5 and 6 to test effects of obstructions*

Control Volume	Test Case 1	2	3	4	5	6
1	0.98[a]	0.92[a]	1.00[c]	0.94[c]	0.80[e]	0.87[e]
2	0.91[a]	0.94[a]	0.98[c]	0.90[c]	0.78[e]	0.90[e]
3	0.75[a]	0.87[a]	0.81[c]	0.85[c]	0.86[e]	0.96[e]
4	0.79[a]	0.91[b]	0.84[c]	0.86[c]	0.93[e]	1.12[f]
5	1.51[a]	1.33[b]	1.36[c]	1.60[d]	0.76[e]	0.98[f]
6	0.94[a]	0.91[a]	0.90[c]	0.98[c]	0.88[e]	1.00[f]
7	0.94[a]	0.91[a]	1.00[c]	0.94[c]	0.92[e]	1.05[f]
8	0.83[a]	0.90[a]	0.92[c]	0.92[c]	1.22[e]	1.30[e]

* For the compared test cases (1 vs 2, 3 vs 4, and 5 vs 6), means with the same superscripts do not differ significantly at 0.05 level of significance.

concentrations tended to be significantly ($p < 0.05$) higher at or near the source than in all the other control volumes at ventilation rates used in the study.

2. Dust generation rate and presence/absence of obstructions (mock pigs) did not significantly ($p < 0.05$) influence the dust concentration distribution.
3. Based on the ASTM (1995) criteria, predicted values agreed well with measured values, especially for the 0.5 to 0.9, 0.9 to 1.6, and 1.6 to 2.8 μm particle diameter size ranges and for total dust. However, measured values of the 2.8 to 5.0 μm particle size range were higher than predicted values.
4. Predicted values indicated that removal by ventilation was the dominant dust removal mechanism (91 to 98% of total dust). Deposition of particles on wall, ceiling and floor surfaces (2 to 9%) was less than removal by ventilation, and effects of coagulation (≈ 0%) were negligible.

Table 6. Comparison of the means of normalized total dust concentrations between test cases 1 and 3, and 2 and 4 to test effects of dust generation rate*

Control Volume	Test Case 1	3	2	4
1	0.98[a]	1.00[a]	0.92[c]	0.94[c]
2	0.91[a]	0.98[a]	0.94[c]	0.90[c]
3	0.75[a]	0.81[a]	0.87[c]	0.85[c]
4	0.79[a]	0.84[a]	0.91[c]	0.86[c]
5	1.51[a]	1.36[b]	1.33[c]	1.60[d]
6	0.94[a]	0.90[a]	0.91[c]	0.98[c]
7	0.94[a]	1.00[a]	0.91[c]	0.94[c]
8	0.83[a]	0.91[a]	0.90[c]	0.92[c]

* For the compared test cases (1 vs 3, 2 vs 4), means with the same superscripts do not differ significantly at 0.05 level of significance.

Table 7. Comparison of the means of normalized total dust concentrations between test cases 3 and 5, and 4 and 6 to test effects of source location*

Control Volume	Test Case 1	3	2	4
1	1.00[a]	0.80[b]	0.94[c]	0.87[d]
2	0.98[a]	0.80[b]	0.90[c]	0.86[c]
3	0.81[a]	0.86[a]	0.85[c]	0.96[c]
4	0.84[a]	0.93[a]	0.86[c]	1.23[d]
5	1.36[a]	0.76[b]	1.60[c]	0.98[d]
6	0.90[a]	0.88[a]	0.98[c]	1.00[c]
7	1.01[a]	0.92[b]	0.94[c]	1.05[d]
8	0.92[a]	1.22[b]	0.92[c]	1.31[d]

* For the compared test cases (3 vs 5, 4 vs 6), means with different superscripts differ significantly at 0.05 level of significance.

FUTURE WORK

Additional research will be conducted to further validate the model. This research will evaluate the effects of other types of ventilation inlets, other types of duct materials, presence of additional obstructions such as pen railings, feed troughs or heating equipment, and other locations of the source in the room.

ACKNOWLEDGMENT. The authors acknowledge the contribution of the following to this research: Dr. William A. Nazaroff, Messrs. Steve Coulson, Darrel Oard, and Cade Schoonover. Contribution No. 99-50-J from the Kansas Agricultural Experiment Station.

REFERENCES

ASTM. 1995. 11.03. Standard guide for statistical evaluation of indoor air quality models (D-5157). In *Annual Book of American Society for Testing Materials Standards*, 484-487. Philadelphia, Pa.

Kato, S., and S. Murakami. 1995. New ventilation efficiency scales based on spatial distribution of contaminant concentration aided by numerical simulation. *ASHRAE Trans.* 94: 309-330.

Liao, C. M., and J. J. R. Feddes. 1992. A lumped parameter model for predicting airborne dust concentrations in a ventilated airspace. *Transactions of the ASAE* 35(6): 1973-1978.

Maghirang, R. G., and H. B. Manbeck. 1993. Modeling particle transport in slot-inlet ventilated airspaces. *Transactions of the ASAE* 36(5): 1449-1459.

Maghirang, R. G., H. B. Manbeck, and V. M. Puri. 1994. Numerical simulation of particle transport in slot-inlet ventilated airspaces. *Transactions of the ASAE* 37(5): 1607-1612.

MWPS. 1990. MWPS-32. Mechanical ventilating systems for livestock housing. Ames, Iowa: Midwest Plan Service.

Nazaroff, W. W., and G. R. Cass. 1989. Mathematical modeling of indoor aerosol dynamics. *Environ. Sci. & Technol.* 23(2): 157-166.

Puma, M. C. 1998. Modeling of dust concentration distribution in swine houses. Unpub. Ph.D. diss. Manhattan, Kans.: Kansas State University.

Worley, M. S., and H. B. Manbeck. 1995. Modeling particle transport and airflow in ceiling inlet ventilation systems. *Transactions of the ASAE* 38(1): 231-239.